

EFFECT OF ROUGHNESS ON THE INTERFACE IN NATURAL FIBRE COMPOSITES: PHYSICAL ADHESION AND MECHANICAL INTERLOCKING

C. A. Fuentes^{a*}, G. Brughmans^b, L.Q.N Tran^a, C. Dupont-Gillain^c,
I. Verpoest^a, A.W. Van Vuure^a

^aDepartment of Metallurgy and Materials Engineering (MTM), KU Leuven, Leuven, Belgium

^bUnit Matter, GROUP T - Leuven Engineering College, Leuven, Belgium

^cInstitute of Condensed Matter and Nanosciences, Université Catholique de Louvain, Louvain-la-Neuve, Belgium

*Carlos.Fuentes@mtm.kuleuven.be

Keywords: Natural-Fibers, Pull-Out, Physical-Adhesion, Interface

Abstract

Physical adhesion was experimentally determined by measuring contact angles with different liquids on bamboo and glass fibers, using the Wilhelmy technique and by applying the acid-base theory for calculating the surface energy components and the theoretical work of adhesion. The mechanical strength of the interfaces was assessed by single fibre pull-out tests. In order to consider the real mechanisms of interfacial failure of natural fibre composites, the fibre matrix interfacial bond strength was characterized by the critical local value of interfacial shear stress, τ_d , and the radial normal stress at the interface, σ_{ult} , at the moment of crack initiation. Both interfacial parameters are used for correlating thermodynamic work of adhesion and practical adhesion. Pull-out tests (taking into account friction), XPS, ToF-SIMS, and profilometry techniques were used to study the influence of rough natural fibre surfaces on the interface between the fibre and a thermoplastic matrix, by comparing the mechanical behaviour at the interface of a smooth optical glass fibre with that of rough natural fibres.

1. Introduction

With the increasing demand for natural fibre reinforced composites, a lot of effort is put in improving their mechanical properties. The weakest part of these composites is often the fibre-matrix interface due to a bad compatibility between the typically hydrophilic reinforcing fibre and in particular hydrophobic thermoplastic matrices. To achieve a composite with good mechanical properties, a strong fibre-matrix adhesion has to be obtained by interfacial interactions, including mechanical interlocking, chemical bonding and physical adhesion.

A quantitative estimation of physical adhesion is possible by wetting analysis, while mechanical and chemical interactions can only indirectly be estimated from destructive micromechanical tests (micro-indentation, pull-out, fragmentation, microdroplet debonding, etc.). However, micromechanical experiments measure “practical adhesion”, which not only represents purely physical and chemical interactions at the interface. Certainly, the load transfer between the fibre and the matrix also depends on the mechanical properties of both,

the fibre and the matrix, and can also be affected by local stresses, matrix residual stresses (processing conditions), presence of easy fracture sites, and the mode of applying external stresses [1, 2]. Hence, micromechanical tests not only measure surface interactions but interdependent interface characteristics.

It is possible to assess the mechanical strength of interfaces by single fibre pull-out tests. The fibre matrix interfacial bond strength was characterized by the critical local value of interfacial shear stress, τ_d . The latter is parallel (mode II) to the fibre surface while the work of adhesion (W_a) is perpendicular (mode I). Since during crack initiation in the pull-out test, the crack surfaces move directly apart, it is possible to correctly relate W_a with the normal stress at the debond point. This radial normal stress at the interface at the moment of crack initiation is used in this study as a parameter for correlating thermodynamic work of adhesion and practical adhesion.

The aim of this publication is to study the influence of physical adhesion and roughness on the mechanical behaviour of interfaces between a glass fibre and a polypropylene (PP) and a polyvinylidene fluoride (PVDF) matrix. Optical glass fibres possess a very smooth surface, and constant cross section along the fibre direction, which make them ideal for reducing the effect of mechanical interlocking. Physical adhesion was experimentally determined by measuring contact angles with different liquids using the Wilhelmy technique and by applying the acid-base theory for calculating the surface energy components and the wetting parameters. Finally, the mechanical behaviour at the interface of the smooth optical glass fibre was compared with that of rough bamboo fibres.

2. Materials and methods

2.1. Materials

The silica core (diameter: 200 μm) of an optical glass fibre from Thorlabs (FR200UMT) was used in this study. Technical bamboo fibres of the species *Guadua angustifolia* were mechanically extracted from bamboo culms in the Department of Metallurgy and Materials Engineering at KU Leuven. Polypropylene and polyvinylidene fluoride (Solef 1008) were obtained from Propex, and Solvay respectively in the form of films.

2.2 Materials preparation

The cladding layer that protects the optical fiber was removed by submerging the fibres in hot sulphuric acid. The fibres were further rinsed off with water and submerged in piranha solution (mixture of concentrated sulphuric acid and hydrogen peroxide) for 30 minutes. Finally, the glass fibres were rinsed off with water again and stored in ultrapure water (resistivity $> 18\text{M}\Omega\cdot\text{cm}$) for avoiding environmental carbon contamination.

Bamboo fibres were cleaned with warm water for one hour (90°C), then wiped with ethanol with a piece of cotton tissue before being dried in a vacuum oven at 80°C for one hour.

2.3 Contact angle measurements and wetting analysis

Advancing and receding contact angles of various test liquids (with different surface energy components) were measured on the polymer films under controlled conditions (temperature of 20°C and humidity of 60%), with a Krüss K100 tensiometer using the Wilhelmy technique

[1]. The average of the cosines of the advancing (θ_{adv}) and receding (θ_{rec}) angles was used for the glass fibres to estimate the cosine of the equilibrium angle (θ_{equ}), as has been suggested by Andrieu et al. [2], and is shown in Equation 1.

$$\cos \theta_{equ} = 0.5 \cos \theta_{adv} + 0.5 \cos \theta_{rec} \quad (1)$$

For the case of bamboo fibres, equilibrium contact angles were measured directly by using acoustic vibration. For applying sound vibrations, an audio speaker (8 Ohm) with an outer diameter of 8.4 cm was mounted in the Krüss K100 tensiometer. The experiments were performed on a vibration-isolated optics table (PFA52509 SuperDamp from Thorlabs).

A wave-file for the frequency sweeps and amplitude profiles was generated by a computer using the Audacity audio editor enabling preparation and control of the cycles in advance. The magnitude of the frequencies depends on the characteristics of the solid and the liquid used during the experiment, since each system needs different amounts of energy to escape from the metastable state.

2.4 Surface characterization: X-ray photoelectron spectroscopy (XPS)

XPS analyses were performed on a Kratos Axis Ultra spectrometer (Kratos Analytical Manchester – UK) equipped with a monochromatized aluminium X-ray source (powered at 10 mA and 15 kV). More information regarding the XPS analysis procedure can be found in [1].

2.5 Pull-out test

Glass and bamboo fibres were embedded in a cylindrical block of polymer with a radius of 5 mm. When the polymer was completely molten, the fibre was placed perpendicular to the polymer surface and in its centre. The specimen was cooled down at a rate of 4°C/min until it reached room temperature. The processing temperatures used were 200°C for PP and 220°C for PVDF.

To perform the pull-out test, the sample was attached to the load cell of an Instron 5943 mini tensile testing machine. A fibre free length of 5 mm was chosen for all the specimens.

2.7 Evaluation of the interfacial strength

Based on the shear lag model of stress transfer to the matrix, Zhandarov et al. [3, 7] have developed a model to describe the current applied force, F , as a function of the crack length, a , for a partially debonded fibre during a pull-out test:

$$F = \frac{\pi d}{\beta} \left\{ \tau_d \tanh[\beta(l_e - a)] - \tau_T \tanh[\beta(l_e - a)] \tanh \left[\frac{[\beta(l_e - a)]}{2} \right] + \beta a \tau_f \right\} \quad (2)$$

Where τ_d is the interfacial shear strength, τ_T is the residual stress due to thermal shrinkage, τ_f is the frictional stress in the already debonded region, l_e is the embedded length, and β is the shear-lag parameter according to Nayfeh [3].

Due to the difference between the coefficients of thermal expansion of the fibre and the matrix, the latter accumulates residual stress during cooling from processing temperatures. This stress compresses the fibre in the radial direction, affecting the interfacial strength.

$$\tau_T = \frac{\beta r_f E_f}{2} (\alpha_f - \alpha_m) \Delta T \quad (3)$$

Where E_f is the longitudinal tensile modulus of the fibre, r_f is the radius of the fibre, and α_f and α_m are the longitudinal coefficients of thermal expansion (CTE) of the fibre and the matrix respectively.

The total debonding of the fibre from the matrix occurs at the recorded peak force F_{max} (see Figure 1). The force up to that moment reflects a combined resistance from friction in already debonded areas and adhesion in the still adhered section. The value of F_{max} can be used to obtain τ_d and τ_f by fitting experimental data according to the algorithm developed by Zhandarov et al. [4]. The variational mechanical analysis of stresses in embedded single fibres, according to Scheer and Nairn [5-7], is used to calculate the normal stress, σ_{rr} , at the moment of crack initiation (σ_{ult}).

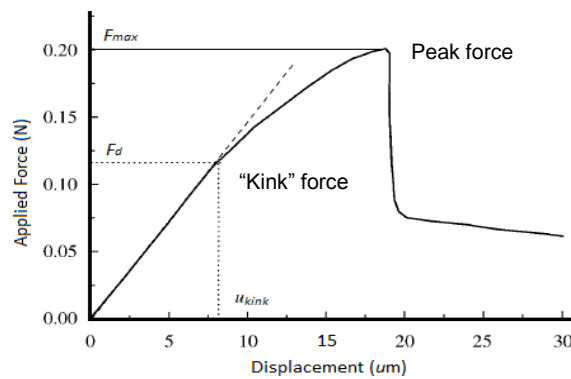


Figure 1. A pull-out test force-displacement curve showing a “kink” at debonding force F_d and peak force F_{max} according to Zhandarov [8].

3. Results and discussion

3.1 Wetting behaviour of glass fibres

Both receding and advancing contact angles of water on cleaned glass fibres vary over time, as can be seen in Figure 2. When contact angles were measured immediately after cleaning, the values were remarkably lower if compared with those after two or three hours. Hence, receding and advancing contact angles of 15 and 36 degrees respectively were measured right after the cleaning procedure, but when the same fibre was exposed to a normal environment and the angles measured one day later, stable receding and advancing contact angles of 50 and 80 degrees were obtained.

This phenomenon is related to the interaction of OH groups on the surface of the fibre with organic molecules from the air and the high surface energy of glass. After the cleaning procedure with sulphuric acid and piranha solution, a group of fibres were stored in ultra-pure water (resistivity $> 18M\Omega.cm$) for protecting them against contamination and another group were exposed to normal environmental conditions.

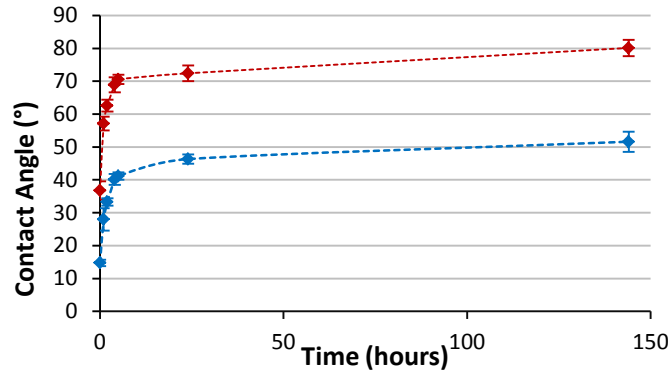


Figure 2. Variation of the advancing (red curve) and receding contact angles (blue curve) of water on clean glass fibre as a function of time.

3.2 Surface energy components

Table 1 shows the results of the contact angle measurements for glass fibres. The equilibrium contact angle is approximated by using the semi-empirical mean of cosines approach as described in 2.3. The calculated surface energy components according to the acid-base model are shown in Table 2.

Material	γ^{tot} (mJ/m ²)	γ^{LW} (mJ/m ²)	γ^+ (mJ/m ²)	γ^- (mJ/m ²)
Bamboo	45.3 ± 1.2	43.2 ± 1.0	0.1 ± 0.0	14.5 ± 1.2
Glass	40.5 ± 2.1	29.7 ± 0.2	1.1 ± 0.2	27.3 ± 0.1

Table 1. Advancing, receding, and equilibrium contact angles for glass fibres.

Contact angle(°)	Water	Ethylene glycol	Diiodomethane
Advancing	36.5 ± 1.4	41.3 ± 2.0	61.8 ± 1.7
Receding	23.1 ± 0.5	20.2 ± 2.6	54.2 ± 1.5
Equilibruim	30.5 ± 1.1	32,2 ± 2.1	58.1 ± 1.6

Table 2. Surface energy components of glass fibre. The surface energy components of bamboo correspond to those reported in our previous publication [9]. The total surface energy ($\gamma_{s,l}$) is divided into a Lifshitz-van der Waals ($\gamma_{s,l}^{\text{LW}}$), an acid ($\gamma_{s,l}^+$) and a base ($\gamma_{s,l}^-$) component.

Table 3 shows the calculated wetting parameters: work of adhesion (W_a), spreading coefficient (S), wetting tension (ΔF), and interfacial energy (γ_{sl}), for bamboo and glass fibres as substrates, following equations 4, 5, 6, 7.

$$W_a = \gamma_s + \gamma_l - \gamma_{sl} = \gamma_l(1 + \cos \theta) \quad (4)$$

$$S = \gamma_s - (\gamma_l + \gamma_{sl}) \quad (5)$$

$$\Delta F = \gamma_s - \gamma_{sl} = \gamma_l \cos \theta \quad (6)$$

$$\gamma_{sl} = \gamma_s^{\text{LW}} + \gamma_l^{\text{LW}} + 2 \left[(\gamma_s^+ \gamma_s^-)^{1/2} + (\gamma_l^+ \gamma_l^-)^{1/2} - (\gamma_s^{\text{LW}} \gamma_l^{\text{LW}})^{1/2} - (\gamma_s^+ \gamma_l^-)^{1/2} - (\gamma_s^- \gamma_l^+)^{1/2} \right] \quad (7)$$

For bamboo fibres, the PVDF-bamboo system gave the best performance showing a higher W_a than PP-bamboo, as well as a positive S value and a low γ_{sl} , helping to achieve a better wetting of the molten polymer on the bamboo fibre.

Material	W_a (mJ/m ²)	S (mJ/m ²)	γ_{sl} (mJ/m ²)	ΔF (mJ/m ²)
PP+bamboo	75.27 ± 1.45	13.53 ± 1.45	0.91 ± 0.57	44.40 ± 1.17
PVDF+bamboo	81.71 ± 1.43	12.42 ± 1.43	-1.75 ± 0.51	47.06 ± 1.29
PP+glass	66.00 ± 0.99	4.26 ± 0.99	5.37 ± 0.35	35.13 ± 1.30
PVDF+glass	70.76 ± 0.76	1.48 ± 0.76	4.38 ± 0.28	36.12 ± 0.36

Table 3. Wetting parameters for bamboo and glass as substrates.

For glass fibres, the PVDF-glass fibre system gives the highest values for W_a and ΔF , and the lowest γ_{sl} , representing the best combination of wetting parameters if compared with PP as a matrix. However, S in PVDF is low, meaning that the molten matrix would have difficulties to spread on the fibre's surface during the impregnation process.

3.3. Pull-out test

Physical and mechanical properties of the fibres and matrices used are listed in Table 4. The determined interfacial parameters and the theoretical work of adhesion (W_a) are shown in Table 5.

	Tg °C	Tc °C	Tm °C	CTE 10 ⁻⁶ /K	Young's modulus GPa	Shear modulus MPa
PP	-25	115.7	160.6	70	1.6	533
PVDF	-30	142.5	174.0	120	2.6	2100
Glass fiber	/	/	/	5	46.6	15000
Bamboo	/	/	/	60*	40.0	1500*

Table 4. Properties of the fibres and matrices used. *Lignin properties [10].

Fiber	Matrix	τ_d (MPa)	τ_f (MPa)	β_{cor}	σ_{ult} (MPa)	W_a (mJ/m ²)
Untreated glass	PP	7.9	2.9	1.16	31.09	66.00
Untreated glass	PVDF	37.0	1.4	2.26	86.76	70.76
Bamboo	PP	3.8	2.7	1.02	12.85	75.27
Bamboo	PVDF	13.8	3.3	1.89	20.11	81.71

Table 5. Interfacial parameters determined from the pull-out test.

There was a good correlation between the interfacial parameters determined from the pull-out test and the theoretical W_a for glass as substrate. As it can be seen in Table 5, the value of τ_d for the PVDF-glass fibre system is approximately 5 times higher than the values obtained for the PP-glass system. The latter clearly indicates a higher interfacial adhesion and greater surface energy components compatibility of PVDF on untreated glass fibres if compared with the PP system, as described in 3.2. If the three glass fibre systems are analysed together, the obtained τ_f value for the PVDF is lower than that for PP (see Table 5).

Even though the roughness of the fibres was the same for the 2 glass systems, the effect of friction is lower in PVDF. This may be related to the difficulty of PVDF to spread on the glass surface due to its low spreading coefficient (see Table 3), reducing the amount of area in contact with the glass surface and also reducing the mechanical interlocking, as the matrix does not penetrate that well into the surface roughness.

As can be seen in Table 5, τ_d values for bamboo fibre are relatively low if compared with glass fibre systems, while τ_f values are relatively high. The latter indicates that friction plays a major role in bamboo fibre systems: debonding occurs at relatively low forces but friction keeps increasing F_{max} , giving the appearance of good mechanical interfacial properties. Contrary to glass systems, the τ_f value obtained for the PVDF-bamboo fibre system is higher than that for bamboo-PP, which may be related to the difference in roughness. In the latter case of bamboo, PVDF may be able to impregnate more surface area due to the relatively big cavities on the fibre surface and the good physical interaction with the fibre, increasing the level of polymer-fibre contact area.

Contrary to expectations, τ_d values are lower for bamboo as substrate than those found for glass, although Wa is higher for bamboo. These results are consistent with those of Thomason [11] and suggest that natural fibres are not able to deliver the level of stress and load distribution efficiency at the interface that would be expected from their high longitudinal mechanical properties. These results may be explained by the anisotropic nature of natural fibres, and particularly bamboo in this study, that provokes a great reduction of their transversal mechanical properties.

For further analysis, the adhesional pressure (σ_{ult}) was used as criteria for interfacial failure. According to Zhandarov [12], this normal stress component at the matrix interface corresponds to the tensile mechanism of crack initiation, and it is directly proportional to Wa , but considers the mechanical properties of the fibre and the matrix. As it can be seen in Table 5, σ_{ult} corresponds well with Wa if the analysis is made independently for each fibre.

However, if bamboo and glass systems are compared, again the performance of bamboo is poor. These findings further support the idea of the anisotropic nature of bamboo fibres as the main cause for its low interfacial properties. Even though the chemistry of the surface of the fibre displays good interaction with the matrix, apparently low transversal mechanical properties fail to transfer stress at the interface. This may be related to the limited mechanical properties of lignin which is predominant at the surface [1].

4 Conclusions

Practical adhesion in single fibre glass and bamboo composites was evaluated by two different interfacial parameters obtained from pull-out tests: τ_d and σ_{ult} . Both parameters are consistent with the theoretical Wa , if each system (glass and bamboo) is independently analysed. As expected PVDF systems give the best interfacial performance due to high physical interaction between the fibre and the matrix.

When bamboo and glass systems are compared, both interfacial parameters (τ_d and σ_{ult}) show a poor performance for bamboo composites, even though Wa is higher for bamboo. Taken together, these results suggest that the physical and chemical compatibility between the bamboo fibre and the matrix may not be improving substantially the composite performance if compared with glass composites.

The anisotropic nature of natural fibres is suggested as the main reason for the low stress transfer capability at the fibre-matrix interphase. Furthermore, the pull-out process may be friction-dominated in bamboo fibre systems.

References

- [1] C.A. Fuentes, L.Q.N. Tran, C. Dupont-Gillain, W. Vanderlinden, S. De Feyter, A.W. Van Vuure, I. Verpoest, Wetting behaviour and surface properties of technical bamboo fibres, *Colloids and Surfaces A: Physicochemical and Engineering Aspects*, 380 (2011) 89-99.
- [2] C. Andrieu, C. Sykes, F. Brochard, Average spreading parameter on heterogeneous surfaces, *Langmuir*, 10 (1994) 2077-2080.
- [3] A.H. Nayfeh, Thermomechanically induced interfacial stresses in fibrous composites, *Fibre Science and Technology*, 10 (1977) 195-209.
- [4] S.F. Zhandarov, E. Mäder, O.R. Yurkevich, Indirect estimation of fiber/polymer bond strength and interfacial friction from maximum load values recorded in the microbond and pull-out tests. Part I: local bond strength, *Journal of Adhesion Science and Technology*, 16 (2002) 1171-1200.
- [5] J.A. Nairn, A variational mechanics analysis of the stresses around breaks in embedded fibers, *Mechanics of Materials*, 13 (1992) 131-154.
- [6] J. Nairn, Generalized shear-lag analysis including imperfect interfaces, *In other words*, 10 (2004) 1.
- [7] R.J. Scheer, J.A. Nairn, Variational mechanics analysis of the stresses in microdrop debond specimens, (1991).
- [8] S. Zhandarov, E. Mäder, Peak force as function of the embedded length in pull-out and microbond tests: effect of specimen geometry, *Journal of Adhesion Science and Technology*, 19 (2005) 817-855.
- [9] C.A. Fuentes, L. Tran, M. Van Hellemont, V. Janssens, C. Dupont-Gillain, A. Van Vuure, I. Verpoest, Effect of physical adhesion on mechanical behaviour of bamboo fibre reinforced thermoplastic composites, *Colloids and Surfaces A: Physicochemical and Engineering Aspects*, (2012).
- [10] C. Baley, Analysis of the flax fibres tensile behaviour and analysis of the tensile stiffness increase, *Composites Part A: Applied Science and Manufacturing*, 33 (2002) 939-948.
- [11] J. Thomason, Why are natural fibres failing to deliver on composite performance?, in: 17th International Conference on Composite Materials, ICCM17, 2009.
- [12] S. Zhandarov, Y. Gorbatkina, E. Mäder, Adhesion pressure as a criterion for interfacial failure in fibrous microcomposites and its determination using a microbond test, *Composites Science and Technology*, 66 (2006) 2610-2628.